A Pan-African age for the HP-HT granulite gneisses of Zabargad island: implications for the early stages of the Red Sea rifting

Joël Lancelot, Delphine Bosch

A Pan African age for the HP-HT granulite gneisses of Zabargad island: implications for the early stages of the Red Sea rifting

Joël R. Lancelot and Delphine Bosch

Laboratoire de Géochimie Isotopique, U.R.A. 13-71, Département des Sciences de la Terre et de l'Univers, U.M. II, Place E. Bataillon, 34095 Montpellier Cedex 5, France

Received July 25, 1991; revision accepted September 16, 1991

ABSTRACT

Up to now the age of granulite gneisses intruded by the Zabargad mantle diapir has been an unsolved problem. These gneisses may represent either a part of the adjacent continental crust primarily differentiated during the Pan African orogeny, or new crust composed of Miocene clastic sediments deposited in a developing rift, crosscut by a diabase dike swarm and gabbroic intrusions, and finally metamorphosed and deformed by the mantle diapir. Previous geochronological results obtained on Zabargad island and Al Lith and Tihama-Asir complexes (Saudi Arabia) suggest an Early Miocene age of emplacement for the Zabargad mantle diapir during the early opening of the Red Sea rift. In contrast, Sm-Nd and Rb-Sr internal isochrons yield Pan African dates for felsic and basic granulites collected 500–600 m from the contact zone with the peridotites. Devoid of evidence for retrograde metamorphic, minerals from a felsic granulite provide well-defined Rb-Sr and Sm-Nd dates of 655 ± 8 and 699 ± 34 Ma for the HP-HT metamorphic event (10 kbar, 850 °C). The thermal event related to the diapir emplacement is not recorded in the Sm-Nd and Rb-Sr systems of the studied gneisses; in contrast, the development of a retrograde amphibolite metamorphic paragenesis strongly disturbed the Rb-Sr isotopic system of the mafic granulite. The initial $^{143}Nd/^{144}Nd$ ratio of the felsic granulite is higher than the contemporaneous value for CHUR and is in agreement with other Nd isotopic data for samples of upper crust from the Arabian shield. This result suggests that source rocks of the felsic granulite were derived at 1.0 to 1.2 Ga from either an average MORB-type mantle or a local 2.2 Ga LREE-depleted mantle. Zabargad gneisses represent a part of the disrupted lower continental crust of the Pan African Afro-Arabian shield. During early stages of the Red Sea rifting in the Miocene, these Precambrian granulites were intruded and dragged upwards by a rising peridotite diapir.

1. Introduction

Zabargad island (23°36.5′N, 36°12′E) is located on the western margin of the northern Red Sea axial trough (Fig. 1). This small island (4 km^2) provides a remarkable laboratory for studying the early stages of Red Sea rifting within the Afro-Arabian shield. Modelling of geophysical data collected over the marine area adjacent to Zabargad suggested the presence of an unserpentinized peridotite body (density of about 3.3–3.4 g/cm^3) extending at least 8 km below the island [1]. Early geological surveys of Zabargad [2–4] augmented by several recent studies provide detailed petrological and geochemical analyses of the three main intrusive and/or metamorphic formations: the peridotite bodies [5–11], the surrounding gneisses [7,12–14], and the diabase dike swarm [7,15]. Microstructural studies of peridotites and gneisses [7,13], documented an asthenospheric uprise related to the early stage of Red Sea rifting; deformation in the gneisses increases towards the peridotites.

Few geochronological data are available to constrain the age of Zabargad diapir emplacement (Table 1). Large excesses of ^{40}Ar make it difficult to date Zabargad amphiboles by K-Ar or Ar-Ar methods [6,7,16,17]. Nevertheless, Nicolas et al. [7] reported a K-Ar date of 23 ± 7 Ma on amphibole, which was interpreted as a maximum age for diapir emplacement. This Miocene age is in agreement with an attempt to date the asthenospheric intrusion using the U-Pb method on zircons extracted from two gneiss samples collected close to the contact zone with the peridotites [18]. For one sample, the U-Pb data pro-

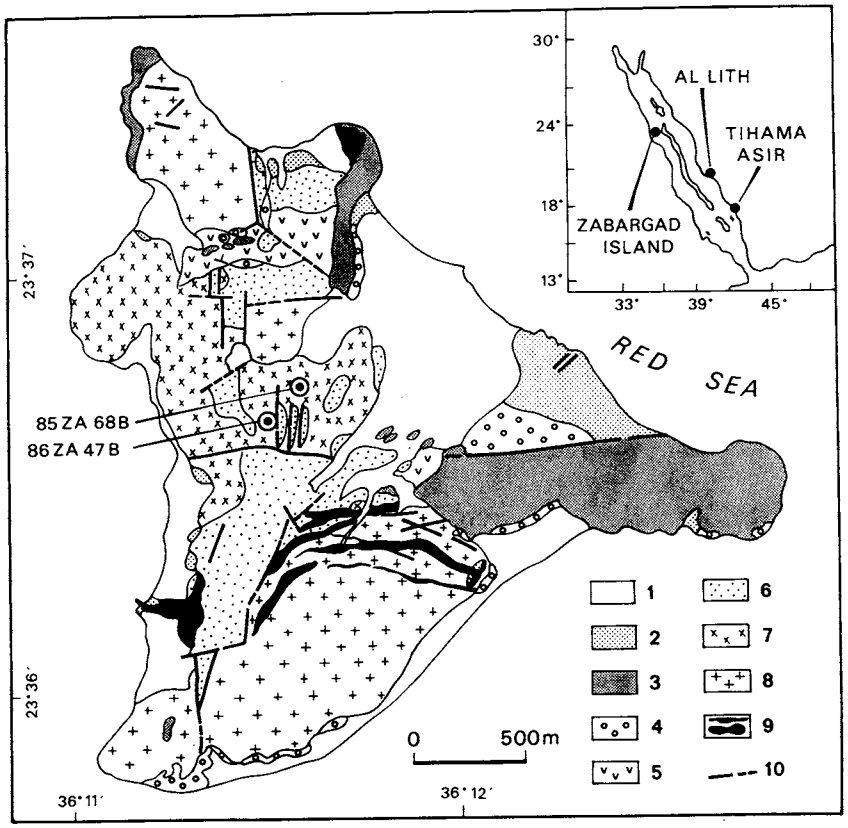

Fig. 1. Geological map of Zabargad island, taken from [2,5,8,13]. *1* = beach sand and recent alluvium; *2* = Late Pleistocene reef limestone; *3* = Pliocene/Early Pleistocene reef limestone; *4* = beach conglomerate; *5* = Upper Miocene evaporite; *6* = Cretaceous or Miocene Zabargad metasedimentary formation; *7* = gneiss unit; *8* = peridotite; *9* = diabase dikes and shallow mafic intrusions; 10 = faults. The locations of 86ZA47B and 85ZA68B are shown.

vide subconcordant points on Concordia diagram with 19–21 Ma dates. Zircon fractions from the other gneiss show an evident inherited component and provide an upper intercept date of 143 ± 11 Ma (Table 1) which is rather difficult to interpret (Jurassic–Cretaceous igneous activity [18]?, U/Pb multistage evolution of detrital zircons?). Nevertheless, all recent studies [1,5,7] emphasized the similarity of Zabargad peridotites with ultramafic bodies from the Atlantic and Indian oceans (mid-oceanic fracture zones, passive continental margins such as the Galicia Bank) and proposed an Early Miocene emplacement age of the peridotite diapir during early stages of Red Sea rifting. The hypothesis that Zabargad mafic and ultramafic rocks were part of a Precambrian ophiolitic sequence [3] is now obsolete, but the origin and the age of the gneisses are still very much a matter for debate. With the exception of the U-Pb study on zircon performed to date the diapir emplacement [18], no radiometric dates have been published for these rocks. The gneisses may represent: (1) Pan African or pre-Pan African formations of the upper continental crust similar to amphibolite-gneiss complexes of the Egyptian Eastern Desert [2,5,7,8,14,19], (2) metamorphosed recent rift sediments and mafic intrusions constituting a new crust of Miocene age formed above the mantle diapir [7,20], or (3) components of the lower continental crust, to which recent mafic intrusions were added by underplating processes during the asthenospheric upwelling [13,14].

To evaluate these three hypotheses, we have

TABLE 1

Previous geochronological data

Rock type	Analyzed mineral	Method	Age (Ma)	References	Remarks
Amphib-olite	Green amphibole	K-Ar	23 ± 7	[6,7]	Sample located 300 m from the contact zone with the peridotites
Gneiss	Green amphibole	K-Ar	65 ± 27	[7]	Sample located 10 m from the contact zone with the peridotites
Gneiss	Zircon	U-Pb	19–21 (Pb-Pb ages)	[18] (abstract)	Nine subconcordant points. Sample from the contact zone with peridotites of the central body
Gneiss	Zircon	U-Pb	90–120 (Pb-Pb ages)	[18] (abstract)	Three discordant points. Sample from the contact zone with peridotites of the central body. The twelve U-Pb data provide a discordia line with intercepts of 18.4 ± 1 and 143 ± 11 Ma
Dolerite Z 2137	Green amphibole	Ar-Ar [a] K-Ar [b]	20.2 ± 3 45	[16,17]	Ar-Ar saddle-shaped spectrum. Dike cutting the gneisses west of the central peridotite body
Peridotite Z 2119	Green amphibole	Ar-Ar [a] K-Ar [b]	65.9 ± 0.9 238	[16,17]	Ar-Ar saddle-shaped spectrum. Sample from the northern peridotite body
Pyroxenite Z 2089	Green amphibole	Ar-Ar [a] K-Ar [b]	32.2 ± 0.8 107.2	[17]	Ar-Ar saddle-shaped spectrum. Sample from the northern peridotite body
Gneiss Z 2155	Green amphibole	Ar-Ar [a] K-Ar [b]	36 ± 1.2 64.4	[17]	Ar-Ar saddle-shaped spectrum. Sample from west of the central peridotite body

[a] Minimum age of the saddle-shaped spectrum.
[b] "Total age" identical to a K/Ar age.

obtained Sm-Nd and Rb-Sr radiometric dates on the gneiss unit intruded by the asthenospheric diapir.

2. Geological background

Three peridotite bodies outcrop on Zabargad island (Fig. 1). These are composed of spinel lherzolite and spinel pyroxenite, deformed and partially recrystallized to a plagioclase-bearing assemblage. Amphibole peridotites are present in the three bodies. The peridotites intrude a gneiss unit located in the central and western parts of the island (Fig. 1); this unit consists of banded amphibolites interlayered with felsic gneisses. Increasing deformation towards the peridotite bodies is clearly expressed in the gneisses [13].

The peridotites and the gneisses are overlain by the folded Zabargad metasedimentary formation, dominantly composed of sandstones and black shales. A widespread diabase dike swarm crosscuts the peridotites, the gneisses and the base of the Zabargad formation. In the northern part of the island this metasedimentary formation is overlain by an Upper Miocene gypsum deposit which is separated by an angular unconformity from overlying beach conglomerates and Pliocene–Pleistocene coral reefs; all are cut by normal faults.

3. Sample description

Detailed microprobe analyses [13,14], of Zabargad gneisses demonstrated a polyphase metamorphic evolution. Two granulite samples —86ZA47B and 85ZA68B— were selected for the geochronological study. They were previously studied to determine the peak metamorphic conditions (10 kbar, 850 °C) and the evolution of the metamorphism [13]. Sample locations are indicated in Fig. 1. The felsic granulite (86ZA47B) contains garnet, orthopyroxene, plagioclase, biotite and quartz with accessory rutile, ilmenite and graphite. In this sample, rare breakdown of

garnet to orthopyroxene-cordierite symplectites suggests a late decompression stage at high temperature under anhydrous conditions. The mafic granulite (85ZA68B) is composed of garnet, clinopyroxene, plagioclase and quartz. However, retrograde reactions typical of the amphibolite facies are widespread in this sample. They include abundant Cl-hydrous minerals developed under static conditions [13]. This suggests interaction with a hydrous, Cl-rich fluid phase, probably seawater. The two granulite samples were not collected in the vicinity of the contact zone with the peridotites (Fig. 1) where reheating at temperatures of 875–900 °C induced by diapir emplacement has overprinted the primary HP-HT assemblage of Zabargad gneisses [13,14].

4. Analytical techniques

Each sample was ground in a stainless steel mortar and split into two parts: one was saved for mineral separation and the other was used for whole rock analyses. Chunks were reduced to a grain size of about 200 μm in a SPEX tungsten carbide crusher, and the powder rinsed with distilled water.

Plagioclase, pyroxene, garnet and biotite were separated using magnetic and gravimetric means. Mineral separates were hand-picked under a binocular microscope and ultrasonically cleaned several times in distilled water. The Sm-Nd and Rb-Sr data were obtained using techniques described previously [21,22]. The total procedural blank was less than 0.15 ng for Nd, 0.17 ng for Sr, and 0.08 ng for Rb. All the isotopic data were obtained on a VG Sector mass spectrometer. Sr was loaded with a Ta activator on a single W filament. Sr ratios were normalized to $^{86}Sr/^{88}Sr = 0.1194$. Nd was loaded onto the Ta side filament of a triple filament assembly with a Re ionizing filament. Nd ratios were normalized to $^{146}Nd/^{144}Nd = 0.72190$. During the course of this study NBS 987 and JMC 361 standards were repeatedly run. Mean measured values were 0.710247 ± 14 (2σ) and 0.511141 ± 16 (2σ), respectively. Initial $^{143}Nd/^{144}Nd$ ratios are commonly expressed in ϵ_{Nd} notation [23].

5. Results

Sm-Nd isotopic data for the felsic granulite 86ZA47B are listed in Table 2. On an isochron diagram (Fig. 2) they form a linear array with a good spread in Sm/Nd ratios. Regression analysis [24] yields a date of 681 ± 33 Ma and a $^{143}Nd/^{144}Nd$ initial ratio of 0.512011 ± 41 (MSWD = 0.818). The Rb-Sr isotopic data on the same sample are listed in Table 2 and shown in Fig. 3. In contrast to the Sm-Nd data they are rather scattered. With respect to Rb-Sr, biotite

TABLE 2

Rb-Sr and Sm-Nd analytical data

Rock type	Sample	Rb (ppm)	Sr (ppm)	Sm (ppm)	Nd (ppm)	$^{87}Rb/^{86}Sr$	$^{87}Sr/^{86}Sr$	$^{147}Sm/^{144}Nd$	$^{143}Nd/^{144}Nd$
Felsic granulite 86ZA47B	Whole rock	25.85	116.9	2.15	7.89	0.6400 ± 0.006	0.71203 ± 0.00003	0.160 ± 0.002	0.51274 ± 0.00002
	Plagioclase	4.82	118.5	0.94	7.82	0.1180 ± 0.009	0.70884 ± 0.00004	0.072 ± 0.001	0.51225 ± 0.00008
	Orthopyroxene	0.251	53.85	3.74	8.64	0.0150 ± 0.001	0.70618 ± 0.00004	0.259 ± 0.003	0.51320 ± 0.00011
	Garnet	0.346	1.19	3.21	2.42	0.8360 ± 0.045	0.71374 ± 0.00006	0.819 ± 0.008	0.51562 ± 0.00015
	Biotite	55.52	10.96	–	–	14.6900 ± 1.59	0.73519 ± 0.00004	–	–
Mafic granulite 85ZA68B	Whole rock	0.294	44.35	1.10	3.90	0.0480 ± 0.002	0.70398 ± 0.00002	0.166 ± 0.002	0.51254 ± 0.00001
	Plagioclase	0.335	83.21	–	–	0.0120 ± 0.001	0.70331 ± 0.00003	–	–
	Clinopyroxene	0.231	71.71	1.90	3.50	0.0091 ± 0.0005	0.70287 ± 0.00003	0.322 ± 0.002	0.51313 ± 0.00001
	Garnet	0.087	2.73	3.90	3.50	0.0930 ± 0.005	0.70553 ± 0.00009	0.679 ± 0.006	0.51439 ± 0.00004

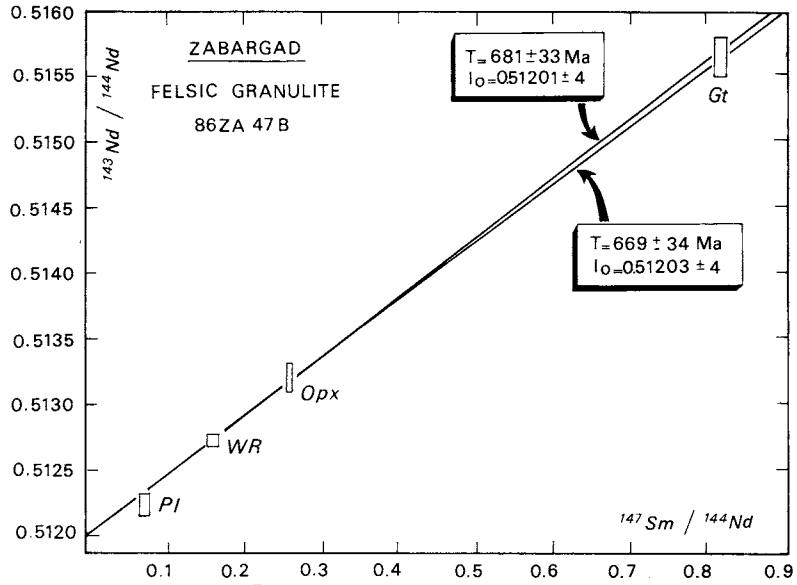

Fig. 2. Sm-Nd isochron plot for minerals and whole rock from 86ZA47B. The two regression analyses yield: $T = 681 \pm 33$ Ma, $(^{143}Nd/^{144}Nd)_0 = 0.51201 \pm 4$, $\epsilon_{Nd0} = +5.2$, MSWD = 0.82 (Pl, WR, Opx, Gt), and $T = 669 \pm 34$ Ma, $(^{143}Nd/^{144}Nd)_0 = 0.51203 \pm 4$, $\epsilon_{Nd0} = +5.3$, MSWD = 0.08 (R, Opx, Gt).

and plagioclase evolved as open systems, and were partially reset during a later event. Rb-Sr data for whole rock, orthopyroxene and garnet appear undisturbed on the other hand, and yield a Pan African date of 655 ± 8 Ma with a $^{87}Sr/^{86}Sr$ initial ratio of 0.70604 ± 3 (MSWD = 0.078). Taking into account the Rb-Sr open system evolution of the plagioclase and that this mineral plots

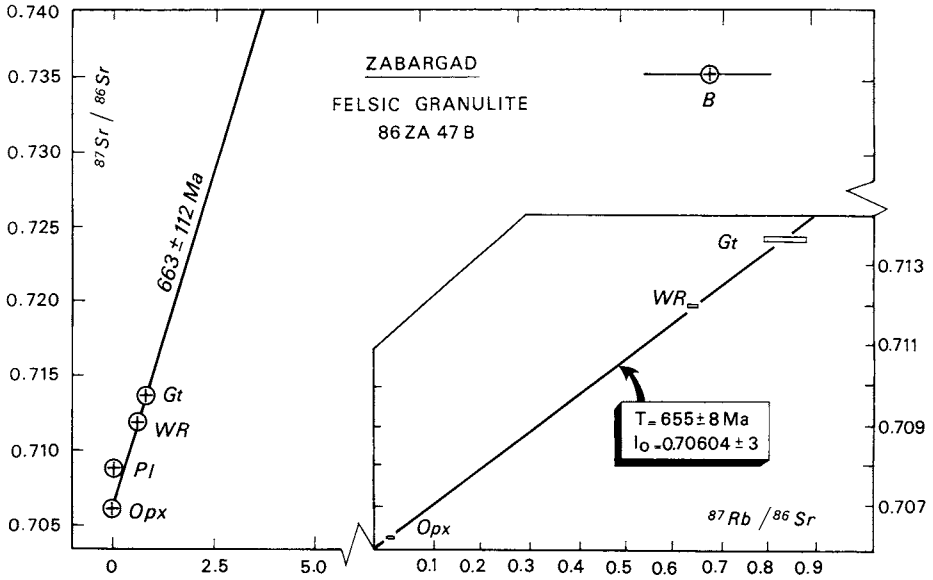

Fig. 3. Rb-Sr isochron plot for minerals and whole rock from 86ZA47B. Inset is an enlarged area of the isochron (Opx, WR, Gt) which yields an age of 655 ± 8 Ma with an initial $^{87}Sr/^{86}Sr$ ratio of 0.70604 ± 3 (MSWD = 0.078).

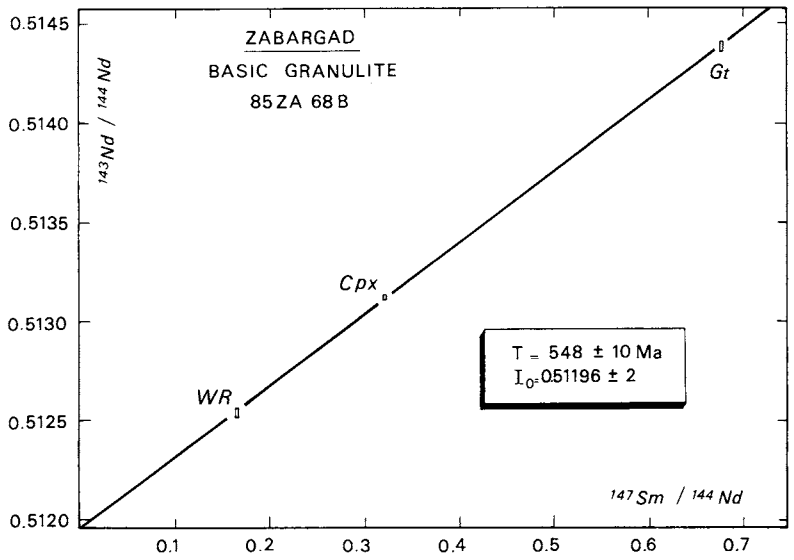

Fig. 4. Sm-Nd isochron plot for whole rock and minerals (Cpx, Gt) from 85ZA68B. Regression analysis yields an age of 548 ± 10 Ma (M.S.W.D. = 1.51) with an initial $^{143}Nd/^{144}Nd$ ratio of 0.51196 ± 2 ($\epsilon_{Nd0} = +0.9$).

slightly below the Sm-Nd internal isochron (Fig. 2), another Sm-Nd isochron was calculated using Opx-Gt-WR data (Fig. 2). This isochron gives a date of 669 ± 34 Ma (MSWD = 0.08) with a $^{143}Nd/^{144}Nd$ initial ratio of 0.512034 ± 44. We note the good agreement of Sm-Nd and Rb-Sr ages using Opx-Gt-WR data of the felsic granulite 86ZA47B.

Sm-Nd isotopic data for the Zabargad mafic granulite 85ZA68B are reported in Table 2. On a Sm-Nd isochron diagram (Fig. 4), they define a linear array with a good spread in Sm/Nd ratios.

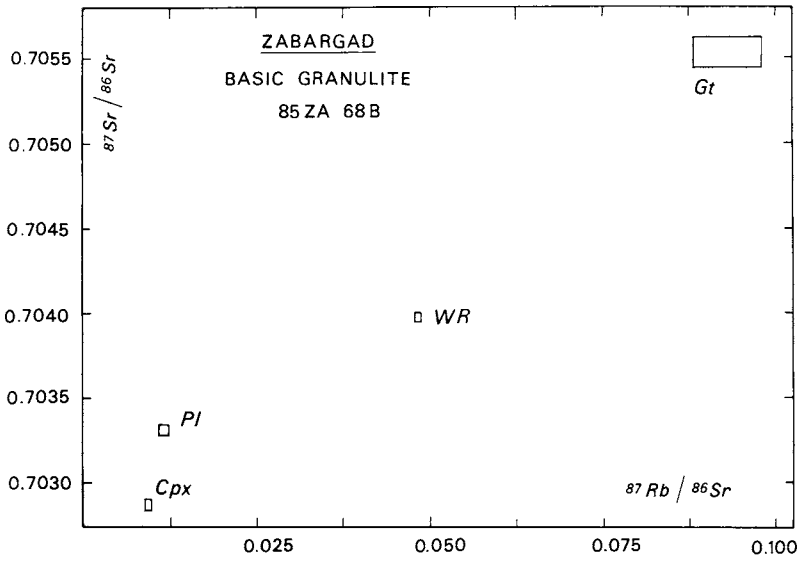

Fig. 5. Rb-Sr isochron plot for whole rock and minerals from 85ZA68B. Scattered experimental points indicate the opening of Rb-Sr systems related to the development of a retromorphic static paragenesis in this basic granulite [13].

Using the three data points (WR, Cpx, Gt), a regression analysis [23] yields a date of 548 ± 10 Ma (MSWD = 1.51) and a $^{143}Nd/^{144}Nd$ initial ratio of 0.51196 ± 2. Rb-Sr isotopic data for 85ZA68B are listed in Table 2. Plotted on a Rb-Sr isochron diagram (Fig. 5) they do not define a linear array. We relate the opening of the Rb-Sr systems to the development of a retrograde static paragenesis in this mafic granulite [13]. Clinopyroxene is partly replaced by actinolite. Coronitic reactions around garnet produce an assemblage of secondary plagioclase (An 62), Fe and Cl-rich amphibole (up to 5% Cl), Cl-rich biotite (up to 2% Cl) and magnetite (C. Mevel, pers. commun.). This suggests interaction with a hydrous Cl-rich fluid phase, probably seawater [13,15,25,26]. Thus, strong disturbances of the Rb-Sr isotopic systems of the mafic granulite may be expected; in addition, development of fine-grained retrograde metamorphic phases in this rock makes it difficult to obtain pure mineral separates.

6. Discussion

6.1. Sm-Nd and Rb-Sr ages

The felsic and mafic components of Zabargad gneisses yield Pan African Sm-Nd dates and where sampled 500–600 m from observable contact zones with the peridotite bodies. The felsic granulite 86ZA47B contains a mineral assemblage devoid of retrograde static paragenesis and records similar dates both by Sm-Nd (669 ± 34 Ma) and Rb-Sr (655 ± 8 Ma) dating on whole rock and separates of garnet and orthopyroxene. According to Sr and Sm diffusion data [27] high closure temperature of pyroxene, favors that isotopic variations due to in-situ radioactive decay are preserved at a mineralogical scale in a granulite after its crystallization, especially if later thermal events occurred in the absence of a fluid phase. The very similar Sm-Nd and Rb-Sr mineral ages found for the Zabargad felsic granulite should be very close to that of the HP-HT crystallization event because homogenization of $^{87}Sr/^{86}Sr$ and $^{143}Nd/^{144}Nd$ initial ratios can easily be achieved for granulite facies conditions [27]. Thus, we conclude that the Pan African age of 660 Ma dates the HP-HT granulite facies metamorphism, physical conditions of which (10 kbar, 850 °C) have been previously established by detailed microprobe analyses on the same sample [13]. For the plagioclase in 86ZA47B, the Rb-Sr isotope chronometer clearly evolved in an open system. A similar evolution, but less disturbed, is also likely for the Sm-Nd system (Figs. 2 and 3). Shifts of plagioclase compositions from the Sm-Nd and Rb-Sr internal isochrons are related to the sensitivity of each isotopic "clock" to a later thermal event. Regression analyses of data points including WR, Gt, Opx and Pl still provide Pan African dates both by Sm-Nd (681 ± 33 Ma, MSWD = 0.82) and Rb-Sr (663 ± 112 Ma, MSWD = 150) methods, but the high values of both experimental error and MSWD lead us to reject this later Rb-Sr date.

The Rb-Sr system of the biotite in 86ZA47B is probably the most affected by a recent thermal event (Fig. 3); the WR-biotite pair indicates a date of 116 ± 5 Ma ($(^{87}Sr/^{86}Sr)_0 = 0.7110$). These data could document the closure age of the WR-biotite system of the felsic granulite during a Cretaceous thermal event [28] which could be related to a pre-Miocene alkaline magmatic activity, preceding the opening of the Red Sea rift. This hypothesis is supported by the occurrence of brown Ti-pargasite or kaersutite and Ti-rich phlogopite in some Zabargad peridotites from the northern and central massifs [9,11] and by widespread alkaline intrusions of Late Cretaceous or Eocene age which crosscut the Pan African basement of the Eastern Desert of Egypt (see [29] for references). It should be noted that a Cretaceous or Paleocene age was assumed [8] for the Zabargad metasedimentary formation which overlies the peridotites and the gneisses. This age was proposed on the basis of: (1) correlation with Upper Cretaceous/Paleocene sedimentary formations outcropping in the Eastern Desert of Egypt [18] and in the Northern Sudan coastal plain [30], and (2) the unpublished discovery of a fossil fish "identified as a Teleostean of the Biryformes group of Cretaceous/Paleocene age" (L. Sorbini, pers. commun. in [8]).

In addition, we note the unexplained upper intercept of 143 ± 11 Ma obtained by the U/Pb method on zircons from gneisses of the contact zone with the peridotites [18] (see Table 1).

However, we can also consider that the date of 116 ± 5 Ma yielded by the 86ZA47B WR-biotite

pair has no geological significance and indicates partial opening of the biotite Rb-Sr system during the Miocene thermal event related to diapir emplacement. Previous K-Ar and Ar-Ar data from Zabargad green amphiboles (Table 1) are compatible with a maximum age of 20–23 Ma for their crystallization. This interpretation is complicated by variable amounts of excess ^{40}Ar [16,17] which are at the origin of saddle shaped Ar-Ar age spectra and K-Ar ages older than Miocene for some of these amphiboles [7,16]. In addition, Oberli et al. [18] also suggested a Miocene age for diapir emplacement on the basis of nine subconcordant zircon Pb-Pb ages (19–21 Ma; Table 1). From our field observations, such recrystallized zircons are several mm large and only observed in the contact zone of the gneisses with the peridotites.

The Sm-Nd date of 548 ± 10 Ma obtained for the mafic granulite (Fig. 4) is younger than the 660 Ma date of the HP-HT granulite facies metamorphism measured by Sm-Nd and Rb-Sr methods on the felsic granulite. The widespread development of a recent retrograde metamorphic static paragenesis in this basic granulite may have slightly disturbed the Sm-Nd systems of the analyzed samples (WR, Gt, Cpx).

6.2. Source rocks and crustal evolution

Bokhari and Kramers [31] have combined Nd and Sr isotope and trace element studies of two Late Proterozoic island arc volcanic sequences in Saudi Arabia. A notable conclusion of this work was that initial Nd isotope ratios of these volcanic rocks are higher than those assumed for a MORB-type mantle (see Fig. 6). They suggested the existence of a local unusually LREE-depleted mantle, in this area, with differentiation age expressed as T^{ND}_{CHUR} of 2.2 Ga [32]. In addition, Nd and Sr isotope determinations on Late Precambrian igneous and sedimentary rocks of the Arabian shield [33] have confirmed Nd initial ratios higher than the contemporaneous values of CHUR; none of these rocks was derived from crustal components older than 1 or 1.2 Ga.

The initial Nd ratio calculated for the Zabargad felsic granulite 86ZA47B (0.51203 ± 4) is higher than that of the chondritic reservoir CHUR [34] at the time of the Pan African HP-HT metamorphic event (Fig. 6). On the Nd isotope evolution diagram used by Duyverman et al. [33], this Nd initial ratio is within the field defined by the evolution paths of all the upper crustal rocks of Early Proterozoic age from Saudi Arabia (Fig. 6). In agreement with these previous results [33], the source of the granulite 86ZA47B could not have derived from a LREE-depleted upper mantle reservoir before either 1.2 Ga (evolution line for a 2.2 Ga depleted mantle [31]) or 1 Ga (evolution inferred for the mantle source of MORB [21,35]).

The $^{143}Nd/^{144}Nd$ initial ratio calculated for the mafic granulite 85ZA68B clearly differs from that of the Late Proterozoic volcanic rocks from Saudi Arabia [31]; on the Nd isotope evolution diagram (Fig. 6), it plots at an intermediate position between the evolution line for the chondritic reservoir CHUR and the field defined by the evolution lines of Late Proterozoic crustal rocks of the Arabian shield. However, for this mafic

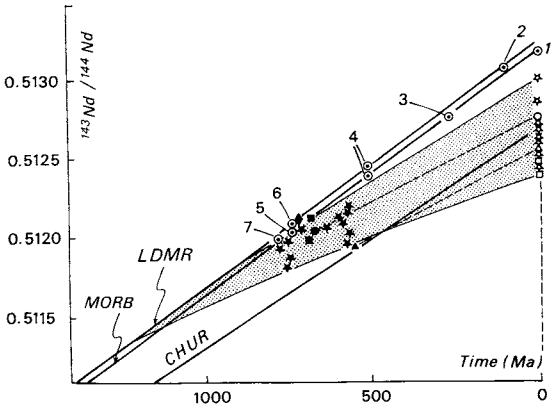

Fig. 6. Variations in initial $^{143}Nd/^{144}Nd$ ratios in samples of Late Proterozoic age from the Zabargad gneiss unit (● = felsic granulite 86ZA47B, ▲ = basic granulite 85ZA68B), and the Arabian shield (◆ and ■ = island arc volcanics [31], ★ = igneous and sedimentary rocks [33]). The shaded area encompasses the evolution lines of all the samples from their intersection with the inferred local 2.2 Ga depleted mantle reservoir [31,33] to their present day value (open symbols). CHUR = evolution line for a chondritic uniform reservoir [30]. LDMR = evolution line for a local depleted mantle reservoir [31] with a differentiation age expressed as T^{Nd}_{CHUR} of 2.2 Ga. MORB = evolution line for the depleted source of mid-ocean ridge basalts [21,35]. ⊙= initial $^{143}Nd/^{144}Nd$ ratios of ophiolites and MORB fall on this line: *1* = MORB [35]; *2* = Oman [35]; *3* = Toba [36]; *4* = Bay of Islands [37]; *5* = Bou Azzer [36]; *6* = Jabal al Wask [38]; *7* = Jabal Ess [38].

granulite the widespread development of retrograde reactions makes it difficult to interpret the Sm-Nd isochron relationship and the low value (0.51196 ± 2) calculated for the initial Nd isotope ratio. Nevertheless, this value could indicate that one part of the Zabargad gneisses was derived from a LREE-depleted mantle before 1.70 or 1.75 Ga, according to the models used for the upper mantle evolution in the concerned area [21,31,35]. This last conclusion may need to be confirmed by additional Sm-Nd data on mafic components of the Zabargad gneisses.

7. Conclusions

7.1. Age of the Zabargad gneiss unit

For the felsic granulite 86ZA47B devoid of retrograde reaction Rb-Sr and Sm-Nd dates of 655 ± 8 and 669 ± 34 Ma respectively demonstrate that the HP-HT metamorphic event (10 kbar, 850 °C) [13] recorded in the mineral paragenesis is Pan African in age. Thus, felsic granulites of the Zabargad gneiss unit represent a component of the lower continental crust differentiated during Pan African orogeny and dragged upwards by the mantle diapir emplaced in the early stages of Red Sea rifting [13,14].

Isotopic analyses performed on the mafic granulite 85ZA68B indicate the opening of the Rb-Sr system in minerals related to widespread retrograde reactions [13,15,25,26]. Nevertheless, the Pan African date of 548 ± 10 Ma obtained by the Sm-Nd method on WR, Cpx and Gt for the mafic granulite suggests that at least one part of the mafic components of the Zabargad gneisses also should be related to Pan African crustal differentiation processes.

These geochronological results rule out the hypothesis of a young crust of Miocene age, composed of recent rift sediments and mafic intrusions metamorphosed and deformed by the mantle diapir [7,20]. In contrast, the occurrence of Pan African granulites on Zabargad is in agreement with the conclusions obtained from geochronological studies of the Eastern Desert of Egypt, the Red Sea Hills of Sudan and Saudi Arabia. These studies document the Late precambrian evolution of the Afro-Arabian shield from island arc to craton and the further Cenozoic disruption of this continental crust by Red Sea rifting. Despite some evidence that small old continental fragments have been added to the crust in this area [39–42], it is now generally agreed that the greatest part of the Afro-Arabian shield developed during the period 900–550 Ma in a sequence of island arcs, followed by plate collision and post-orogenic intracratonic processes [31,33,38,43–52]. Nd and Sr data [31,33,38] indicate that the 900–550 Ma igneous suites exposed in Saudi Arabia and in the Eastern Desert of Egypt were derived from the upper mantle. This rapid crustal growth occurred during Late Proterozoic time without extensive reworking of older continental components.

7.2. Emplacement age of the Zabargad diapir

The thermal event related to diapir emplacement is not clearly recorded in the Sm-Nd and Rb-Sr systems of whole rocks and minerals of the studied granulitic gneisses collected far away from the contact zone with the peridotites. Despite the Cretaceous date yielded by WR and biotite from the felsic granulite, we favor an Early Miocene age of 19–21 Ma for the diapir emplacement on the basis of the U-Pb data from recrystallized zircons collected within the contact zone of gneisses and peridotites [18]. Large and variable amounts of excess ^{40}Ar characterize Zabargad green amphiboles [17], nevertheless K-Ar and Ar-Ar data [6,7,16,17] are compatible with an upper limit of 20–23 Ma for the emplacement age of the diapir. This Early Miocene age is also consistent with K-Ar (from 18.4 ± 3.1 to 24.3 ± 1 Ma [53]) and Ar-Ar dates (from 21 to 24 Ma [54]) obtained on tholeiites of the Al Lith and Tihama Asir complexes located along the western coast of Saudi Arabia (Fig. 1). Diabase dike swarm, layered gabbros, granophyric intrusions, and basaltic lava flows which compose these complexes are considered to have been emplaced during the early opening of the Red Sea rift [53].

The Cretaceous "date" recorded by the WR-biotite pair of the felsic granulite indicates a partial or total resetting of the biotite Rb-Sr system during a recent thermal event which could be related either to the Miocene emplacement of the mantle diapir or to pre-Miocene alkaline magmatic activity, preceding the opening of the Red Sea rift.

Acknowledgements

This work was supported by the D.B.T. program (contracts No. 88 38 02 and 89 38 30) and was carried out while one of us (D.B.) was in recepti of a M.R.T. grant. The authors are grateful to A. Abdel-Monem, D. Ben Othman, J.M. Luck, C. Mevel and B. Nelson for stimulating discussions and useful remarks. We also thank F. Boudier and A. Nicolas for their expert field assistance, both above and below the sea level. R. Montigny and M. Tatsumoto are thanked for their constructive criticism of the paper. Logistical support furnished by Nuclear Material Authority and the Nasr Phosphat Company in Egypt during the 1990 field trip to Zabargad was appreciated. This is CNRS-INSU DBT contribution No. 194.

References

1 P. Styles and K.D. Gerdes, St John's Island (Red Sea): a new geophysical model and its implications for the emplacement of ultramafic rocks in fracture zones and at continental margins, Earth Planet. Sci. Lett. 65, 353–368, 1983.
2 F.W. Moon, Preliminary geological report on St John's Island, Red Sea, Geol. Surv. Egypt, 16 pp., 1923.
3 E.M. El Shazly and G.S. Saleeb, Scapolite-cancrenite mineral association in St John's Island, Egypt, 24th Int. Geol. Congr., Montreal, Rep. Sect. 14, pp. 192–199, 1972.
4 E.M. El Shazly, G.S. Saleeb and N. Zaki, Quaternary basalt in St John's, Red Sea, Egypt, J. Geol. 18, 137–148, 1974.
5 E. Bonatti, P. Hamlyn and G. Ottonello, Upper mantle beneath a young oceanic rift: peridotites from the island of Zabargad (Red Sea), Geology 9, 474–479, 1981.
6 A. Nicolas, F. Boudier, N. Lyberis, R. Montigny and P. Guennoc, L'île de Zabargad (Saint Jean): témoin clé de l'expansion précoce en Mer Rouge, C. R. Acad. Sci. Paris 301/14, 1063–1068, 1985.
7 A. Nicolas, F. Boudier and R. Montigny, Structure of Zabargad Island and early rifting of the Red Sea, J. Geophys. Res. 92, 461–474, 1987.
8 E. Bonatti, R. Clocchiatti, P. Colantoni, R. Gelmini, G. Marinelli, G. Ottonello, R. Santacroce, M. Taviani, A.A. Abdel-Meguid, H.S. Assaf and M.A. El Tahir, Zabargad (St John) Island: an uplifted fragment of sub-Red Sea lithosphere, J. Geol. Soc. London 140, 677–690, 1983.
9 E. Bonatti, G. Ottonello and P.R. Hamlyn, Peridotites from the island of Zabargad (St John) Red Sea: petrology and geochemistry, J. Geophys. Res. 91, 599–631, 1986.
10 H.K. Bruekner, A. Zindler, M. Seyler and E. Bonatti, Zabargad and the isotopic evolution of the Sub-Red Sea Mantle and Crust, Tectonophysics 150, 163–176, 1988.
11 G.B. Piccardo, B. Messigna and R. Vannucci, The Zabargad peridotite-pyroxenite association: petrological constants on its evolution, Tectonophysics 150, 135–162, 1988.
12 E. Bonatti and M. Seyler, Crustal underplating and evolution in the Red Sea rift: uplifted gabbro/gneiss crustal complexes on Zabargad and Brothers islands, J. Geophys. Res. 92, 803–812, 1987.
13 F. Boudier, A. Nicolas, J.R. Kienast and C. Mevel, The gneiss of Zabargad island: deep crust of rift, Tectonophysics 150, 209–227, 1988.
14 M. Seyler and E. Bonatti, Petrology on gneiss-amphibolite lower crustal unit from Zabargad island, Red Sea, Tectonophysics 150, 177–207, 1988.
15 R. Petrini, J.L. Joron, G. Ottonello, E. Bonatti and M. Seyler, Basaltic dykes from Zabargad Island, Red Sea: petrology and geochemistry, Tectonophysics 150, 229–248, 1988.
16 I.M. Villa, $^{40}Ar/^{39}Ar$ analysis of amphiboles from Zabargad island (Red Sea), Tectonophysics 150, 249, 1988.
17 I.M. Villa, $^{40}Ar/^{39}Ar$ dating of amphiboles from Zabargad island (Red Sea) is precluded by interaction with fluids, Tectonophysics, 180, 369–373, 1990.
18 F. Oberli, T. Ntaflos, M. Meier and G. Kurat, Emplacement age of the peridotites from Zabargad island (Red Sea): a zircon U-Pb isotope study, Terra Cognita 7, 334, 1987.
19 N.F. El Ramly, A new geological map of the basement rocks in the Eastern and Southwestern deserts of Egypt, Scale 1/1000000, Ann. Geol. Surv. Egypt 11, 1–18, 1972.
20 A. Nicolas, Novel type of crust produced during continental rifting, Nature 315, 112–115, 1985.
21 D. Ben Othman, Contraintes apportées par les traceurs isotopiques Sm-Nd et Rb-Sr sur la genèse et le développement de la croute continentale, 120 pp, Ph.D. Thesis, Univ. Paris VII, 1982.
22 J.L. Birck, Chronologie primitive des objets planétaires différenciés, 354 pp, Ph.D. Thesis, Univ. Paris VII, 1979.
23 D.J. Paolo and G.J. Wasserburg, The sources of island arcs as indicated by Nd and Sr isotopic studies, Geophys. Res. Lett. 4, 465–468, 1977.
24 J.F. Minster, L.P. Ricard and C.J. Allègre, $^{87}Rb/^{87}Sr$ chronology of enstatite meteorites. Earth Planet. Sci. Lett. 44, 420–440, 1979.
25 P. Agrinier, C. Mevel and M. Javoy, High temperature hydratation of Zabargad peridotites: chemical and isotopic evidences of progressive seawater introduction, Terra Cognita 1, 1, 202, 1989.
26 D. Bosch, Introduction d'eau de mer dans le diapir mantellique de Zabargad (Mer Rouge) d'après les isotopes du Sr et du Nd, C.R. Acad. Sci. Paris 313, II, 49–56, 1991.
27 M. Sneeringer, S. Hart and N. Schimizu, Strontium and samarium diffusion in diopside, Geochim. Cosmochim. Acta 48, 1589–1608, 1984.
28 R.A. Cliff, Isotopic dating in metamorphic belts, J. Geol. Soc. London 142, 97–110, 1985.
29 A.M. Ashad, Present status of geochronological data on the Egyptian basement complex, Proc. Symp. Evolution and mineralization of the Arabian Nubian Shield, Inst. Appl. Geol. (Jeddah) Bull. 3, 31–45, 1980.

30 A.J. Whiteman, The Geology of the Sudan Republic, 256 pp., Clarendon, Oxford, 1971.
31 F.Y. Bokhari and J.D. Kramers, Island arc character and late Precambrian age of volcanics at Wadi Shwas, Hijaz, Saudi Arabia: Geochemical and Sr and Nd isotopic evidence, Earth Planet. Sci. Lett. 54, 409–422, 1981.
32 M.T. Mc Culloch and G.J. Wasserburg, Sm-Nd and Rb-Sr chronology of continental crust formation, Science 200, 1003–1011, 1978.
33 H.J. Duyverman, N.B.W. Harris and C.J. Hawkesworth, Crustal accretion in the Pan African: Nd and Sr isotope evidence from the Arabian Shield, Earth Planet. Sci. Lett. 59, 315–326, 1982.
34 D.J. De Paolo and G.J. Wasserburg, Nd isotopic variations and petrogenetic models, Geophys. Res. Lett. 3, 249–252, 1976.
35 M.T. Mc Culloch, T.T. Gregory, G.J. Wasserburg and H.P. Taylor, Sm-Nd, Rb-Sr and $^{18}O/^{16}O$ isotopic systematics in an oceanic crustal section. Evidence from the Samail ophiolite near Ibra, Oman, J. Geophys. Res. 86, 2721–2735, 1981.
36 P. Richard and C.J. Allègre, Neodymium and strontium isotope study of ophiolite and orogenic lherzolite petrogenesis, Earth Planet. Sci. Lett. 47, 65–74, 1980.
37 S.B. Jacobsen and G.J. Wasserburg, Nd and Sr isotopic study of the Bay of Islands ophiolite complex and the evolution of the source of mid-ocean ridge basalts, J. Geophys. Res. 84, 7429–7445, 1979.
38 S. Claesson, J.S. Pallister and M. Tatsumoto, Samarium-Neodynium data on two late Proterozoic ophiolites of Saudi Arabia and implications for crustal and mantle evolution, Contrib. Mineral. Petrol. 85, 244–252, 1984.
39 A.A. Abdel-Monem and P.M. Hurley, U-Pb dating of zircons from psammitic gneisses, Wadi Abu Rosheid-Wadi Sikait area, Egypt, Proc. Symp. Evolution and mineralization of the Arabian-Nubian Shield, Inst. Appl. Geol. (Jeddah) Bull. 2, 165–170, 1979.
40 J.Y. Calvez, J. Delfour, J. Kemp and E. Elsass, Pre-Pan African inherited zircons from the northern Arabian shield, Saudi Arabian Deputy Minist. for Min. Res. Rep., BRGM-OF-05-13, 22 pp., 1985.
41 J.S. Stacey and C.E. Hedge, Geochronologic and isotopic evidence for early Proterozoic crust in the eastern Arabian Shield, Geology 12, 310–313, 1984.
42 J.S. Stacey and R.A. Agar, U-Pb isotopic evidence for the accretion of a continental microplate in the Zalm region of the Saudi Arabian Shield, J. Geol. Soc. London 142, 1189–1203, 1985.
43 W.R. Greenwood, D.G. Hadley, R.E. Anderson, R.J. Fleck and D.L. Schmidt, Late Proterozoic cratonization in southwestern Saudi Arabia, Philos. Trans. R. Soc. London Ser. A 280, 517–527, 1976.
44 A.E.J. Engel, T.H. Dixon and R.J. Stern, Late Precambrian evolution of Afro-Arabian crust from ocean arc to craton, Geol. Soc. Am. Bull. 91, 699–706, 1980.
45 R.M. Shakelton, A.C. Ries, R.H. Graham and W.R. Fitches, Late Precambrian ophiolitic melange in the Eastern Desert of Egypt, Natue 285, 472–475, 1980.
46 M. Hussein, A. Kroner and S. Durr, Wadi Onib, a dismembered Pan African ophiolite in the Red Sea Hills of Sudan, Proc. Symp. I.G.C.P. Proj. 164, Pan African Crustal Evolution in the Arabian Nubian Shield, Bull. Fac. Earth Sci., King Abdulaziz Univ. 6, 320–327, 1983.
47 M.J. Roobol, N.J. Jackson and D.F. Darbyshire, Late Proterozoic lavas of the Central Arabian Shield: evolution of an ancient volcanic arc system, J. Geol. Soc. London 140, 185–202, 1983.
48 J.S. Stacey, D.B. Stoeser, W.R. Greenwood and L.B. Fischer, U-Pb zircon geochronology and geological evolution of the Halaban–Al Amar region of the Eastern Arabian Shield, Kingdom of Saudi Arabia, J. Geol. Soc. London 141, 1043–1055, 1984.
49 R.J. Stern and C.E. Hedge, Geochronological and isotopic constraints on late Precambrian crustal evolution in the Eastern Desert of Egypt, Am. J. Sci. 285, 97–127, 1985.
50 J.C. Cole and C.E. Hedge, Geochronologic investigation of late Proterozoic rocks in the northeastern Shield of Saudi Arabia, Saudi Arabian Deputy Minist. for Min. Res. Rep. U.S.G.S.-TR-05-5, 42 pp., 1986.
51 J.S. Pallister, J.S. Stacey, L.B. Fischer and W.R. Premo, Precambrian ophiolites of Arabia: geological settings, U-Pb geochronology, Pb isotope characteristics and implications for continental accretion, Precambrian Res. 38, 1–54, 1988.
52 J.S. Pallister, J.C. Cole, D.B. Stoeser and J.E. Quick, Use and abuse of crustal accretion calculations, Geology 18, 35–39, 1990.
53 R.G. Coleman, D.G. Hadley, R.G. Fleck, C.T. Hedge and M.M. Donato, The Miocene Tihama Asir ophiolite and its bearing on the opening of the Red Sea, Proc. Symp. Evolution and mineralization of the Arabian Nubian Shield, Inst. Appl. Geol. (Jeddah) Bull. 1, 173–186, 1979.
54 G. Feraud, V. Zumbo, A. Sebai and H. Bertrand, $^{40}Ar/^{39}Ar$ age and duration of theoliitic magmatism related to the early opening of the Red Sea rift. Geophys. Res. Lett., 18 (2), 195–198, 1991.